Biogeochemistry **9**: 53–74, 1990

Sulfate reduction in fine-grained sediments in the Eastern Scheldt, southwest Netherlands

OENE OENEMA
Netherlands Fertilizer Institute, c/o Institute for Soil Fertility, P.O. Box 30003, 9705 RA Haren, The Netherlands

Key words: sulfate reduction, sulfide accumulation, diffusion, modelling, pyrite

Abstract. Sulfate reduction and sulfide accumulation were examined in fine-grained sediments from rapidly accreting abandoned channels and mussel culture areas in the Eastern Scheldt, which covered 4 and 5% of the total surface area, respectively.

Reduction rates were measured in batch experiments in which the SO_4^{2-} depletion was measured during anoxic incubation. The reduction rates in summer varied between 14–68 mmol SO_4^{2-} m^{-2} day^{-1} and were related to the sedimentation rate. In the most rapidly accreting channels, SO_4^{2-} was exhausted below 15–50 cm and methanogenesis became the terminal process of organic carbon oxidation.

One-dimensional modelling of sulfate profiles in mussel banks indicated that the subsurface influx of SO_4^{2-} was almost of the same order as the diffusive flux at the sediment-seawater interface, during the initial stages of the mussel bank accretion. The energy dissipation of waves and tidal currents on the mussel bank surface increased the apparent sediment diffusivity up to 3-fold, especially in the winter.

The results indicate that acid volatile sulfide (AVS) was the major, in-situ reduced, sulfur compound in the sediment. The sulfidation of easily extractable iron was nearly complete. Pyrite concentrations (40–80 μM S cm^{-3}) were as high as the AVS concentrations, but there was apparently no in-situ transformation of AVS into pyrite. The detrital pyrite originated from eroding marine sediments elsewhere.

Introduction

Bacterial sulfate reduction is an important pathway for organic carbon mineralization in nearshore marine sediments (Jørgensen 1977, 1982; Howarth 1984; Crill & Martens 1987). In this process organic compounds are oxidized and dissolved sulfate is reduced simultaneously by heterotrophic microorganisms. A necessary pre-condition for sulfate reduction is an anoxic environment.

The rate of sulfate reduction in marine sediments is primarily dependent on the amount and reactivity of decomposable organic carbon (Berner 1964; Goldhaber & Kaplan 1975; Lyons & Gaudette 1979; Westrich & Berner 1984). A fair correlation has been observed between the rate of sulfate

reduction and the rate of sedimentation (Goldhaber & Kaplan 1975; Toth & Lerman 1977; Berner 1978; Jørgensen 1982).

Several studies have shown that only a small percentage of the sulfide produced by bacteria is trapped in the sediment as iron sulfide (e.g., Jørgensen 1977; Berner 1984; Howarth 1984; Berner & Westrich 1985). Most of it diffuses upward, and is re-oxidized in the surface layer. The availability of easily reducible iron (Berner 1970; Pyzik & Sommer 1981), bioturbation and the rate of sedimentation (Chanton et al. 1987), all seem to be major influences on sulfide retention.

Thus, with an increase in sedimentation rate, the relative importance of organic carbon mineralization by sulfate reducers and the sulfide retention increase. However, high rates of sulfate reduction cause exhaustion of interstitial sulfate in the subsurface sediment, and under such conditions methanogenesis becomes the terminal process of organic carbon mineralization (Claypool & Kaplan 1974).

The extent of sulfate exhaustion depends on the balance of the reduction rate in the sediment and the transport rate of sulfate from the overlying seawater into the sediment. The latter process seems to be influenced by the sedimentation rate as well, since methane bubble ebullition from methane saturated sediments enhances the solute transport between sediment and overlying seawater (Klump & Martens 1981; Martens & Klump 1980). This, in turn, may affect the total rate of sulfate reduction in rapidly accreting sediments.

This paper reports investigations on bacterial sulfate reduction in fine-grained sediments in the Eastern Scheldt, a tidal inlet in the southwestern Netherlands (Fig. 1). The rate of sulfate reduction, sulfide accumulation and the pore water characteristics in these sediments will be discussed.

Methods

The study sites

Before 1987 the Eastern Scheldt had a surface area of 450 km^2 and an average depth of 8 m. The sediments were predominantly sandy, with low concentrations ($\leqslant 0.1\%$) of organic carbon. Fine-grained sediments were present in mussel culture areas (mussel plots) on 16 km^2 of tidal flats and channels within and below the tide range (Fig. 1). The mussels (*Mytilus edulis L.*) are grown by bottom culture on the sandy surfaces of the tidal flats. Within a period of 6–12 months, they deposited 10–15 cm of faeces rich (1–3%) in organic carbon on the sandy surface of the tidal flats and channel

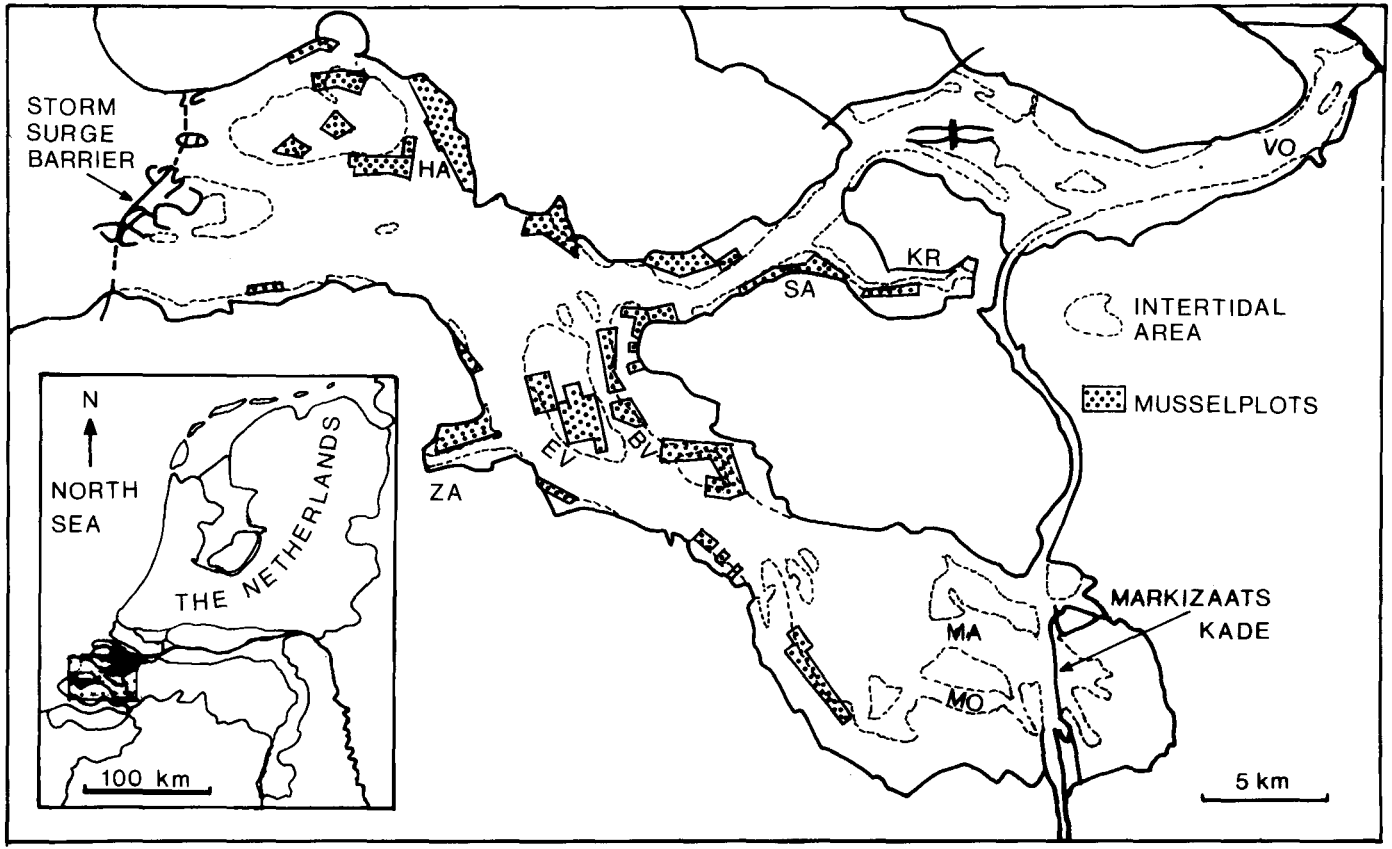

Fig. 1. Location of mussel plots and abandoned channels in the Eastern Scheldt, Southwest Netherlands.

slopes (Oenema 1989). At the end of the 1–2 year growth period, both mussels and mud were removed by dredging. Another depositional environment of fine-grained sediments was present in artificially created abandoned channels, covering approximately 5% of the total surface area of the Eastern Scheldt (Fig. 1). These channels lost much of their tidal discharge after having been cut off within the framework of the 'Delta-Plan' (Knoester et al. 1984).

Mussel banks were sampled at St. Annaland (SA), Zandkreek (ZA) and the Hammen (HA); channel sediments were sampled in the Zandkreek (ZA), Krabbenkreek (KR), Volkerak (VO), Marollegat (MA) and the Mosselkreek (MO) in August 1984–December 1986 (Fig. 1).

Interstitial water analysis

During a period of one year the pore waters from a thick, 1–2 years old mussel bank were sampled at 1–2 month intervals, using the technique of in-situ dialysis (e.g., Hesslein 1976). The in-situ pore water sampler enabled repeated sampling at exactly the same location, as described in detail in Oenema (1988b). This technique was used to avoid the large spatial variation within and between mussel banks. Tests indicated that the concentrations of Cl^- and SO_4^{2-} in the sampler and those in cores taken at a few cm distance from the sampler differed less than 5% after equilibration for 30 days.

Other sites on the intertidal flats were sampled by slowly twisting a PVC tube (i.d. 10 cm) in the sediment. In the channels the cores were taken by divers. Pore water from sediment cores was sampled by a centrifugation technique; 1–3 cm sediment sections were quickly transferred into airtight stoppered tubes, flushed for 5 min with N_2 gas and centrifuged for 5 min, close to the temperature at the sample site.

The pore waters were analyzed by standard auto-analyzer techniques for Cl^- (mercury thiocyanate; Zall et al. 1956), SO_4^{2-} (methylthymol blue; Merks & Sinke 1981) and total dissolved sulfide (ΣS) by methylene blue (Gilboa-Garber 1971). Standard deviations of the SO_4^{2-} determinations varied from 1% at the level of seawater concentration (22 mM) to 5% at 1–2 mM.

Methane concentrations were determined once (December 1986) in cores from abandoned channels. Two ml of sediment was transferred by a decapitated syringe into 25 ml glass vials with butyl rubber stoppers. CH_4 concentrations in the headspace were determined by a gas-chromatograph, 4 days after sampling.

Measurement of sulfate reduction

Rates of sulfate reduction were calculated in $\mu M\ SO_4^{2-}\ cm^{-3}$ wet sediment day^{-1} from the SO_4^{2-} depletion in incubated sediment samples. Sediment sections of 1–3 cm were sampled with 5 ml decapitated syringes and three portions of 23–25 cm^3 were quickly transferred into three 25 ml glass vials fitted with butyl rubber caps. The headspace of the vials was immediately flushed with N_2 gas for 5–10 min. One vial was used for the determination of the initial SO_4^{2-} concentration, the two other vials were incubated in anoxic mud at in-situ sediment temperature for 1–3 weeks. Pore water was obtained by centrifugation. Two ml was transferred into tubes containing 5 ml Zn-acetate (0.4%). After 1–7 days of storage in the refrigerator, these tubes were again centrifuged prior to analysis, to remove any precipitate including zinc sulfides.

Reduction rates were also calculated from the SO_4^{2-} depletion in undisturbed sediment cores in Plexiglas tubes (I.D. 5.6 cm, length 30 cm) sealed in thick-walled, closely fitting PVC tubes and by the radio-tracer technique of Hordijk et al. (1985), with small modifications (Oenema 1988a). The results of the whole core incubations ($78 \pm 31\ mM\ SO_4^{2-}\ m^{-2}\ day^{-1}$) and the radiotracer experiments ($92 \pm 27\ mM\ SO_4^{2-}\ m^{-2}\ day^{-1}$) differed less than 20% from those of the batch experiments ($87 \pm 16\ mM\ SO_4^{2-}\ m^{-2}\ day^{-1}$) in September 1985 (5 cores each). This suggests that the mixing of the sediment in the batch experiments did not significantly affect the rate of SO_4^{2-} reduction.

The rate of SO_4^{2-} reduction was linear during the course of incubation. This was observed during the short term (1–4 hrs) radiotracer experiments, as well as in the batch incubations, following the SO_4^{2-} depletion over 1–2 weeks in summer and 2–8 weeks in winter.

Sediment analysis

Acid-volatile sulfides (AVS) were dissolved after addition of 2 ml 5 M HCl to 2 ml of sediment and trapped into two Zn-acetate traps with N_2 as a carrier gas. The distillation was continued for 1 hr. Extraction with 5 M HCl has been shown to yield slightly lower AVS concentrations than with 5 M HCl + $SnCl_2$, since $SnCl_2$ prevents the oxidation of ΣS by dissolved Fe^{3+} (Chanton & Martens 1985, Morse & Cornwell 1987). The quantity of sulfide so collected, which was analyzed by iodimetric titration (Bassett et al. 1978), may therefore underestimate the total AVS concentration.

Pyrite was determined in oven-dried (80 °C) samples by selective Fe-FeS_2

dissolution (Begheyn et al. 1978). A 1:2 molar Fe/S ratio was used to convert Fe-FeS_2 into S-FeS_2.

Easily reducible iron oxyhydroxides were determined by extraction with NH_4-oxalate (1 M; pH 3) for 4 hr (Schwertmann 1964). The dissolved iron concentration was analyzed by AAS.

Results

Depletion of interstitial sulfate

The slight seasonal salinity gradient in the Eastern Scheldt was reflected almost without time-lag in the variations of the Cl^- and SO_4^{2-} profiles of the sandy sediments from the tidal flats (Fig. 2). This suggests a rapid sediment-seawater exchange in these sediments with very low organic carbon concentrations ($\leqslant 0.1\%$).

The presence of organically-rich debris in mussel banks stimulated bacterial sulfate reduction and caused pore water SO_4^{2-} depletion with depth (Fig. 3). In the sandy sediments below the mud deposits, the SO_4^{2-} concentration was nearly as high as in the overlying seawater. Occasionally, in thick (> 15 cm) mussel banks, SO_4^{2-} was found to be almost exhausted at depths of 10–15 cm, especially in the summer and fall (Fig. 4).

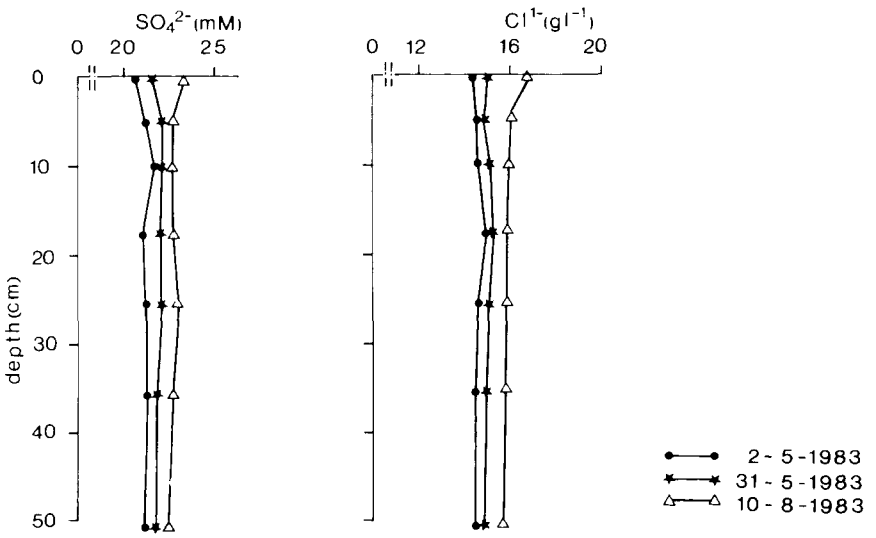

Fig. 2. Seasonal variations in pore water sulfate and chloride concentrations in a sandy sediment ($< 0.1\%$ org. C, $< 5\%$ clay + silt) of the intertidal zone.

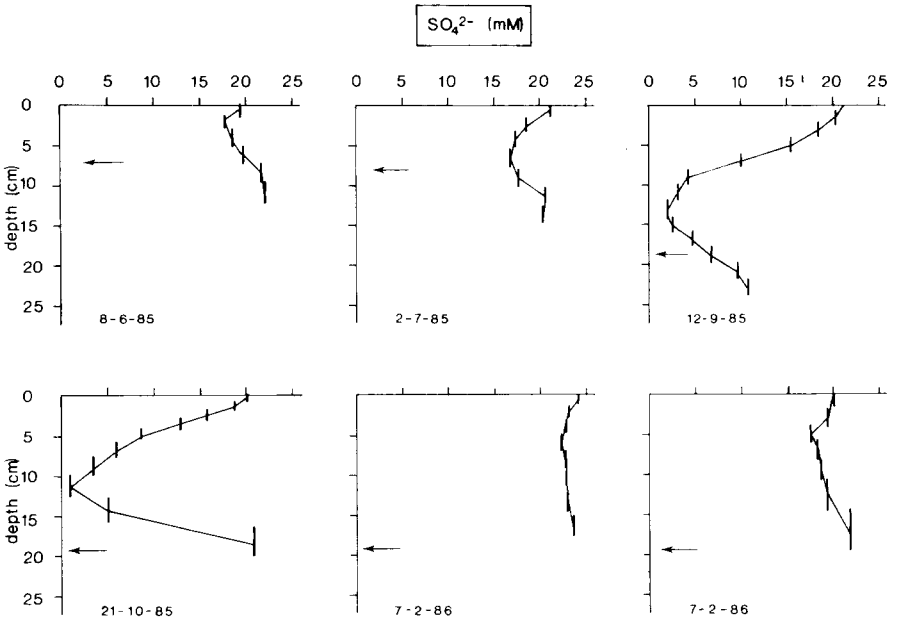

Fig. 3. Pore water sulfate profiles in accreting mussel banks. Arrows indicate depth of mud deposit.

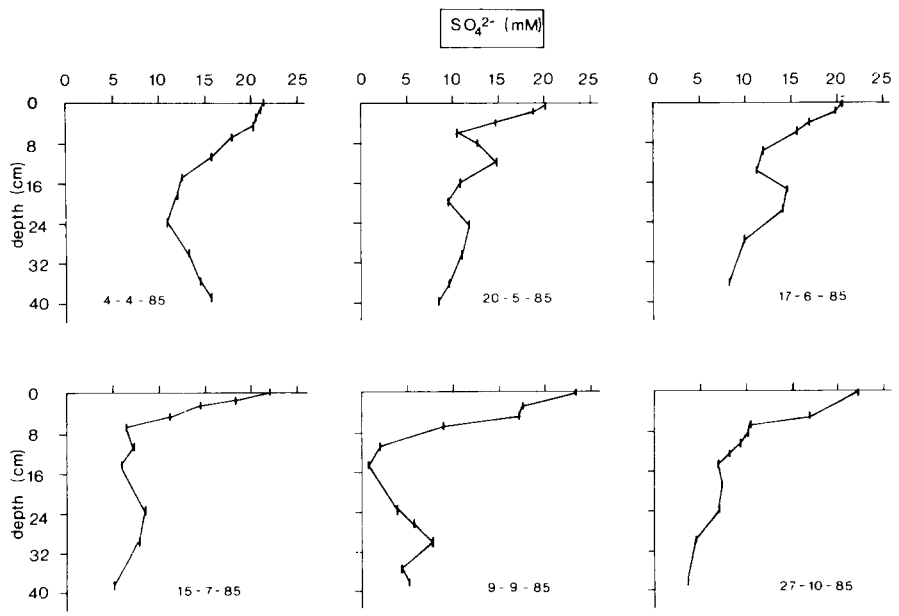

Fig. 4. Seasonal variation in pore water sulfate in a thick, non-accreting mussel bank.

Table 1. Sulfate reduction rates in mussel banks; means and ranges.

Period of sampling	Incubation temp. (°C)	Reduction rates mmol SO_4^{2-} m^{-2} day^{-1}	Number of cores
February	3	7 (3–9)	5
April	8	28 (12–38)	6
July–Sept.	17–20	68 (37–130)	31
October	15	46 (37–87)	6

In recently-abandoned channels, for example in the Mosselkreek, SO_4^{2-} rapidly decreased in the top few cm but increased again near the interface of the shallow mud deposit and the underlying sandy sediments. This phenomenom was also observed in mussel banks less than 1 year old, and implies a flux of SO_4^{2-} from the sandy subsurface towards the overlying fine-grained sediment. Where the thickness of the mud deposits in the channels exceeded 30–60 cm, SO_4^{2-} was exhausted at depths of 15–50 cm (Fig. 5B).

Methane concentrations were low (< 20 nM CH_4 cm^{-3}) in the sediments with pore waters containing SO_4^{2-}. In sulfate-exhausted sediments the pore waters were oversaturated with CH_4 at depths of 7 to 25 cm. Below these depths, the cores were filled with CH_4 bubbles and the CH_4 concentrations varied between 1.5 and 6 μM cm^{-3}.

Sulfate reduction

Mean rates of sulfate reduction in mussel banks are listed in Table 1. Most of the data pertain to the summer and fall, when reduction rates were high, because of high temperatures and thick mussel banks. After the planting of the mussels in early spring, the layer of accumulated faeces increased from

Table 2. Means and standard deviations of sulfate reduction rates (mmol SO_4^{2-} m^{-2} day^{-1}) in sediments from abandoned channels in September (15–16 °C) and December (8–9 °C) 1986. Means of 3–6 cores.

Location	Sedimentation rate (cm y^{-1})*	Org. C (%)*	Sulfate reduction rate	
			Sept.	Dec.
Volkerak	1.5	1.5	14 ± 3	
	2.5	3.0	32 ± 5	
Krabbenkreek	4	1.5	24 ± 7	10 ± 8
	5	2.5	43 ± 8	10 ± 6
Zandkreek	10	2.5	41 ± 7	27 ± 6
	15	3.5	47 ± 11	28 ± 8
Mosselkreek	5	2.5	37 ± 11	

* from Oenema (1989)

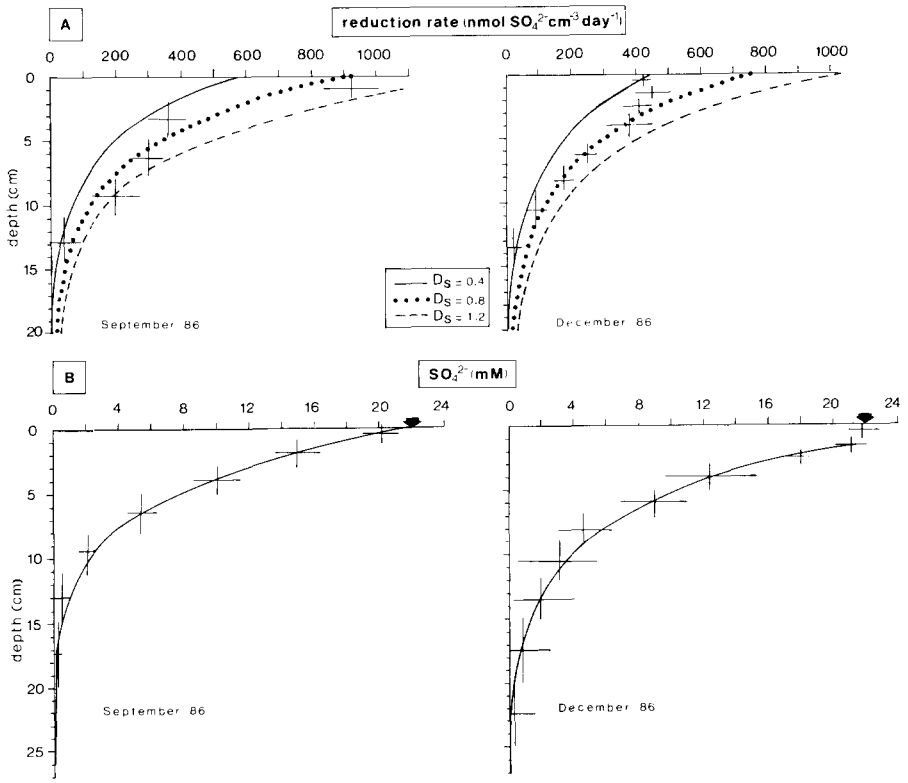

Fig. 5. (*A*) Sulfate reduction profiles and (*B*) sulfate concentration profiles of sediments in the Zandkreek channel. Mean results of 6 cores each; horizontal bars denote ± 1 s.d. Curves are fits with the modified Berner model for various sediment diffusion coefficients (D_s, in $cm^2\,day^{-1}$). Arrows in B denote seawater sulfate concentration. (see Discussion).

essentially zero to 10–15 cm in late fall. The reduction rates were 10–30 mM SO_4^{2-} $m^{-2}\,day^{-1}$ in the shallow mussel banks during early summer, and 40–130 mM SO_4^{2-} $m^{-2}\,day^{-1}$ in the 15 cm thick mussel banks in late summer and fall. Another part of the depth variation is caused by the heterogeneity of the mussel banks (sand-layers, dead mussels, bioturbation by catworms, *Nepthys hombergii*).

Results from the abandoned channels are shown in Table 2. Rates of sulfate reduction decreased with depth, presumably because of substrate limitation and sulfate exhaustion (Fig. 5). Reduction rates were highest at the most rapidly accreting sites, near the end of the channels. The dependence of bacterial sulfate reduction on the supply of easily decomposable organic material is demonstrated by the relation between the mean reduction rates in the top 2 cm and the mean sedimentation rate (Fig. 6).

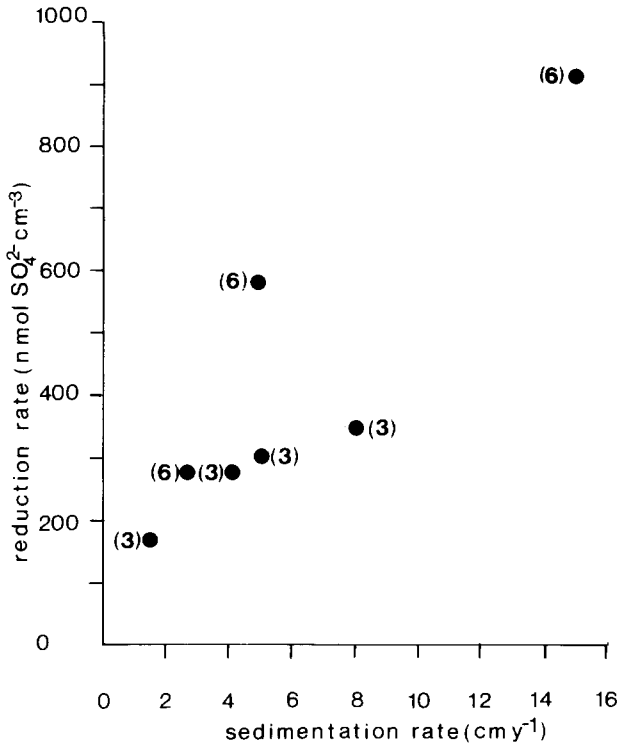

Fig. 6. Sedimentation rates and sulfate reduction rates in the uppermost 2 cm of various abandoned channels in September 1986. Numbers refer to number of replicates.

Sulfide accumulation

In recent mussel banks, the dissolved ΣS concentrations were low (< 0.2 mM). High concentrations (2–8 mM) were observed in 1–2 year old mussel banks (Fig. 7A). Surface layers (0–3 cm) contained little ΣS in autumn and winter, because of stronger wave agitation in these seasons. Concentrations of ΣS were low in the sulfate-exhausted channel sediments, where methanogenesis was the terminal process of organic carbon mineralization (Fig. 7B).

Acid volatile sulfide (AVS) concentrations typically varied between 40–80 μM S cm^{-3} in the black colored muds (Fig. 8). Pyrite concentrations ranged from 30–60 μM S cm^{-3} in mussel banks to 60–100 μM S cm^{-3} in channel sediments. Both pyrite and AVS concentrations varied little with depth (Fig. 8). The oxalate-extractable Fe concentration (Fe_{ox}) varied between 30–65 μM in mussel banks to 80–105 μM Fe cm^{-3} in channel sedi-

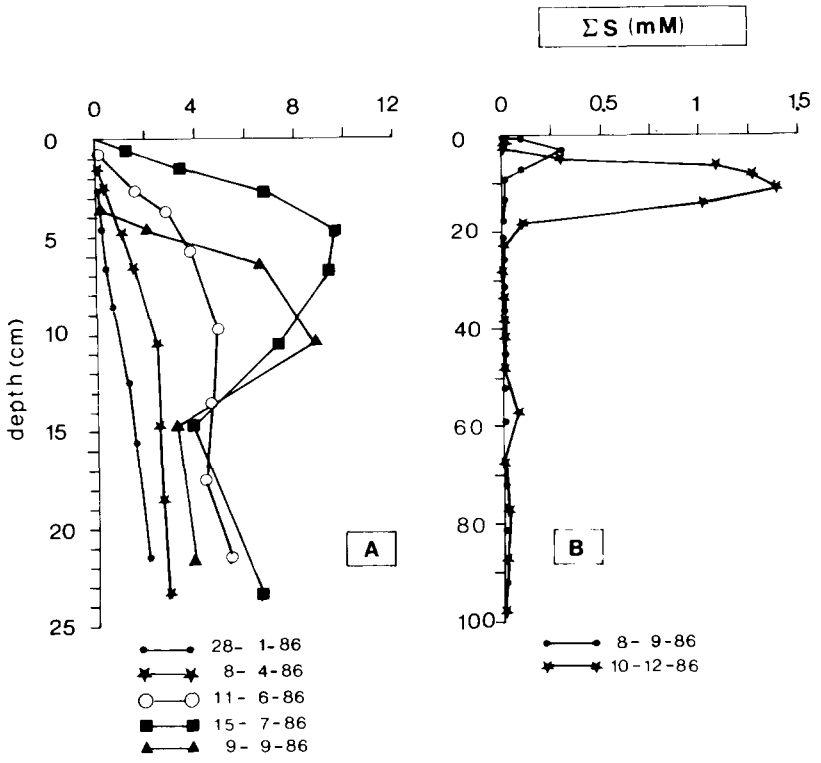

Fig. 7. Total dissolved sulfide in (*A*) 1–2 year old mussel bank and (*B*) in sediments of the Zandkreek. Note the difference in depth scale.

ments. Comparison of the AVS and Fe_{ox} concentrations (the latter included also the iron tied up with AVS) indicated that a large fraction of Fe_{ox} was converted to FeS, especially in mussel banks more than one year old.

Discussion

Rates of sulfate reduction in the fine-grained sediments of the mussel banks and abandoned channels in the Eastern Scheldt were as high as, or higher than, those reported for other near-shore marine coastal sediments (e.g., Skyring 1987). High rates of sedimentation in abandoned channels resulted in complete SO_4^{2-} exhaustion and methanogenesis became the terminal process of organic carbon mineralization. Reduction rates in mussel banks were not limited by SO_4^{2-} exhaustion, even though reduction rates were very high in late summer. Apparently, there was a large influx of SO_4^{2-} into the mussel banks.

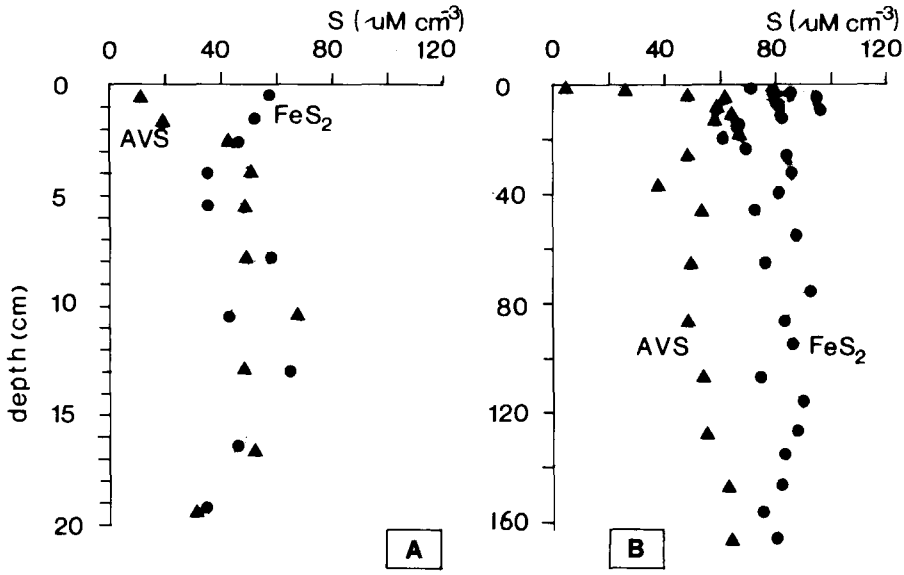

Fig. 8. Acid volatile sulfides (AVS) and pyrite (FeS_2) in (*A*) 1–2 year old mussel bank and (*B*) in sediments of the Zandkreek. Note the difference in depth scale.

Modelling the sulfate profiles in mussel banks

One-dimensional diagenetic models can provide a check for consistency in the measured distributions of dissolved constituents, reaction rates and authigenic minerals (Berner 1980). The changes in pore water SO_4^{2-} with time t at a given depth x below the sediment surface are a function of transport (diffusion, advection, sedimentation) and bacterial sulfate reduction (Berner 1964):

$$\frac{dC}{dt} = D_s \frac{d^2C}{dx^2} - \frac{wdC}{dx} - R_x \qquad (1)$$

where $C = SO_4^{2-}$ concentration ($\mu M\,cm^{-3}$),
$D_s = SO_4^{2-}$ diffusion coefficent ($cm^2\,day^{-1}$),
w = sedimentation rate ($cm\,day^{-1}$), and
R_x = depth dependent rate of SO_4^{2-} reduction ($\mu M\,cm^{-3}\,day^{-1}$).

The main purpose of the following models was to study the SO_4^{2-} transport in the pore waters of accreting mussel banks. A two-layer model was used. In the upper layer, the mussel bank, the change in SO_4^{2-} concentration with time and depth was described by Eq. (1). In the lower layer, the underlying

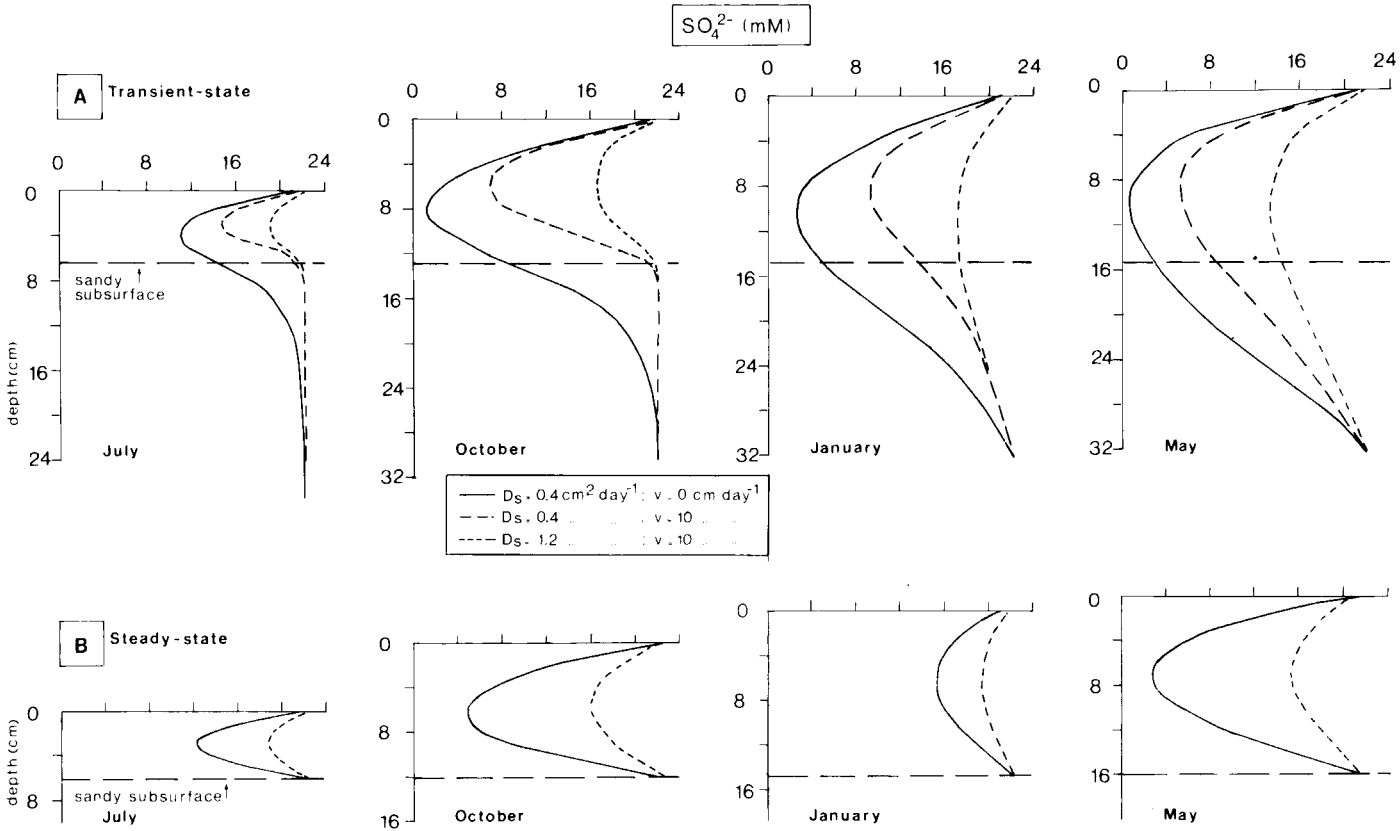

Fig. 9. Simulation of pore water sulfate profiles in an accreting mussel bank. (*A*) two-layer transient-state model (Eq. 1 and 2) and (*B*) one-layer steady-state model (Eq. 4). See Discussion.

sandy tidal flat sediments, the SO_4^{2-} concentration was governed by diffusion and advection only, according to the formula:

$$\frac{dC}{dt} = D_2 \frac{d^2C}{dx^2} + V \frac{dC}{dx} \quad (2)$$

where V = mass flow ($cm\,day^{-1}$), and D_2 = SO_4^{2-} diffusion coefficient in the sandy sediment.

The microbial organic carbon oxidation by sulfate reduction can be adequately described by first-order kinetics (Berner 1964; Westrich & Berner 1984), and the depth dependent rate of SO_4^{2-} reduction by the expression:

$$R_x = R_0 \exp(-bx) \quad (3a)$$

where R_0 = the reaction rate at zero depth, b = attenuation coefficient (cm^{-1}).

A simple sine function was used to correct sulfate reduction rates in the mussel banks for seasonal variations in temperature:

$$R_x = \{R_m + A \sin(2\pi t/365)\} \exp(-bx) \quad (3b)$$

where R_m = mean sulfate reduction rate at zero depth, and A = amplitude.

R_m and A were estimated from the sulfate reduction rate measurements and the Arrhenius law for temperature correction. R_m and A were set at 0.6 and 0.4 $\mu M\,SO_4^{2-}\,cm^{-3}\,day^{-1}$, respectively. The attenuation coefficient b was estimated from the SO_4^{2-} and reduction rate profiles; it varied from 0.1 to 0.3 cm^{-1}.

Equations (1) and (2) were solved numerically using Gear's method (Dew & Walsh 1981) for the following conditions:

initial condition ($t = 0$): $C = C_0$ for $x = 0$ to $x = \infty$

boundary conditions ($t > 0$): $C = C_0$ for $x = 0$

$C = C_0$ for $x = \infty$

Eq. (1) holds for $x = 0$ to $x = wt$

Eq. (2) holds for $x = wt$ to $x = \infty$

$w = 0.07\,cm\,day^{-1}$ for $t < 210$ days

$w = 0.001\,cm\,day^{-1}$ for $t \geq 210$ days

In order to save computer time, the lower boundary was set at x = 32 cm, i.e., twice the maximum thickness of the mussel bank.

The shape of the generated SO_4^{2-} profiles (Fig. 9A) closely resemble the

basic shape of the measured profiles (e.g., Fig. 3). A strong SO_4^{2-} depletion was obtained when annual mean diffusion coefficients ($D_s = 0.4\,cm^2\,day^{-1}$) were used. The diffusion coefficient in sediment, corrected for porosity and tortuosity, was calculated from the diffusion coefficient D in seawater (Li & Gregory 1974), according to $D_s = D\Phi^{n-1}$, with $n = 2$ (Ullmann & Aller 1982) and Φ = porosity (0.6). With the growth of the mussel bank, the SO_4^{2-} depletion increased. The pore waters of the underlying sandy tidal flat sediments also became depleted, because of a diffusive flux towards the depleted pore waters of the mussel banks. After approximately 1 year, the sandy subsurface was almost as depleted as the mussel banks and the upward flux of SO_4^{2-} decreased. In this case, the generated SO_4^{2-} profiles were similar to the measured profiles in the thick, 1–2 year old mussel bank (Fig. 4).

Several important conclusions can be drawn from the behavior of this model. The subsurface SO_4^{2-} flux was almost as large as the sediment-seawater exchange, during the initial stages (< 6 months) of the mussel bank growth. Mass flow of pore water in the sandy sediments increased the importance of the SO_4^{2-} influx from the subsurface and significantly diminished the SO_4^{2-} depletion in the mussel bank (Fig. 9A). There are no measurements of mass flow available, but the possible occurrence of advection was inferred from the almost instantaneous equilibration of the pore water Cl^- concentration in tidal flat sediments whenever seasonal changes in the Cl^- concentration of the overlying seawater occurred (Fig. 2). A change in the apparent sediment diffusion coefficient in the upper layer also had a marked effect on the concentration profiles. This is in accordance with the observations of Jørgensen (1978). Such increases in apparent diffusivities, up to 3-fold, can be caused by waves and tidal currents.

In a simpler one-layer model Eq. (1) was solved for a steady-state situation ($dC/dt = 0$). The analytical solution of Eq. (1) for the boundary conditions:

$x = 0 \qquad C = C_0$

$x = h = wt \qquad C = C_0$ is given in Eq. 4.

$$C_x = C_0 + \frac{R_0}{b^2 D_s + bw} * \frac{1 - \exp(-bh)}{\exp\left(\frac{wh}{D_s}\right) - 1} * \exp\left(\frac{wx}{D_s}\right) - 1 + \exp(-bh) - 1 \quad (4)$$

Results of this model, using data similar to those used for the transient-state model, are shown in Fig. 9B. Again, the basic shape of the generated profiles is

profiles is similar to the measured profiles. There are, however, two major differences with the results of the two-layer transient-state model:

— The one-layer steady-state model does not provide for SO_4^{2-} depletion in the underlying sands. This caused steeper gradients of concentration against depth near the lower boundary and, consequently, a stronger upward-directed flux.

— The response of the SO_4^{2-} profiles to a decrease in reduction rates during the winter (e.g., January profiles) was too slow in reality to establish steady-state conditions readily. Thus, the transient-state model predicted a much stronger SO_4^{2-} depletion than the steady-state model during the winter season. However, measured SO_4^{2-} profiles in winter (Fig. 3) showed a small depletion only. This would indicate that the apparent sediment diffusivity was greater during the winter than during the summer season.

Modelling of SO_4^{2-} reduction in channel sediments

For sulfate-exhausted sediments, Boudreau and Westrich (1984) advocate the use of models that include formulations for the reduction kinetics that are also dependent on the SO_4^{2-} concentration. However, for convenience, a modification of the original Berner (1964) model was proposed. This model excludes the negative SO_4^{2-} concentrations implicit in the original model, by solving Eq. (1) for the following boundary conditions (steady-state conditions):

$$x = 0 \quad C = C_0$$

$$x = z \quad C = 0 \text{ and } dC/dx = 0$$

The solution in dimensional form is as follows:

$$C_x = C_0 - \frac{R_0 D_s}{D_s bw + w^2} * \exp\left(\frac{-D_s bz + wz}{D_s}\right) * \left(1 - \exp\left(\frac{wx}{D_s}\right)\right) - \frac{R_0 \exp(-bx)}{D_s b^2 + wb} \tag{5}$$

where z is the depth of sulfate-exhaustion. R_0 was solved for $x = z$ and $C_z = 0$ to obtain:

$$R_0 = C_0 \Big/ \frac{D_s}{D_s bw + w^2} * \exp\left(\frac{-D_s bz + wz}{D_s}\right) * \left(1 - \exp\left(\frac{zw}{D_s}\right)\right.$$

$$+\left(\frac{1-\exp(-bz)}{D_s b^2+wb}\right) \tag{6}$$

Equation (5) was fitted to the measured SO_4^{2-} profiles to obtain estimates of the SO_4^{2-} exhaustion depth z and the attenuation coefficient b. Results are shown in Fig. 5B. The best fits were obtained for $z = 20$ and $z = 28$ cm in September and December cores, respectively. In order to check that these results were consistent with the measured reduction rates, the appropriate rate equation given in Eq. (3a), was fitted to the measured reduction rate profiles (Fig. 5A), where R_0 is given in Eq. (6). Reasonable fits were obtained with apparent diffusivities of 1–2 times the molecular diffusion coefficient, corrected for porosity (0.83) and tortuosity. The slightly increased apparent diffusivity in the sulfate-exhausted sediments was probably caused by the effects of methane bubble ebullition on solute transport in pore waters (Klump & Martens 1982).

Even though the model described the measured concentration and rate profiles reasonably well, simple steady-state diagenetic equations may not be appropriate for sediments in abandoned channels. The seasonal variations in sedimentation conditions (Oenema 1989) and the possibility of a summer-time subsurface maximum in reduction rates through the upward diffusion of CH_4 (Devol et al. 1984) suggests that the dependence of sulfate reduction on one steady pool of substrate is inaccurate. Note e.g., the decrease in reduction rate in the surface layers of the December vs. September cores (Fig. 5A). Further study is needed to clarify the importance of seasonal variations in substrate sources for sulfate reducers in these channel sediments.

Sulfide accumulation

During the early months of mussel bank accretion, much of the bacterially produced sulfide reacted rapidly with the easily reducible iron oxyhydroxides to form FeS. With increasing height of the mussel banks the net accretion and thus the supply of reducible iron oxyhydroxides slowed down, and high concentrations of dissolved ΣS built up in the pore waters of these thick mussel banks. The large seasonal variation shown in Fig. 7A thus includes both the effect of temperature on rates of ΣS production (e.g., Jørgensen 1977; Crill & Martens 1987) and the effect with time of a diminishing pool of easily reducible iron oxyhydroxides. The concentration of easily metabolizable organic matter also decreased with time, but was apparently still large enough to support high rates of sulfate reduction.

The straight FeS, FeS_2 and Fe_{ox}, profiles (Fig. 8) strongly suggest that the

iron monosulfides were not transformed into the thermodynamically more stable pyrite (Berner 1970, 1984; Sweeney & Kaplan 1973). Formation of FeS_2 would involve the reaction of FeS with reduced sulfur at intermediate oxidation stages, such as elemental sulfur or polysulfides (Berner 1970; Rickard 1975). The concentration and formation rate of these sulfur species are low in reducing sediments (e.g., Howarth & Jørgensen 1984; Luther et al. 1985) and, therefore, may limit in-situ FeS_2 formation via FeS intermediates. Thus, high FeS concentrations will be preserved in the highly reducing mussel banks and channel sediments. These concentrations are up to 3 times the maximum concentrations reported for near-shore marine sediments in the Gulf of California (Goldhaber & Kaplan 1980), Long Island Sound (Aller 1980), Limfjorden (Howarth & Jørgensen 1984; Jørgensen 1977) and Cape Lookout Bight (Chanton et al. 1987). However, in those latter sediments FeS converted to FeS_2 and the FeS concentration rapidly decreased and the FeS_2 concentration increased with depth.

High FeS_2 concentrations were observed in the surface layers of all recent sediments (Fig. 8). Pyrite may form rapidly in surface layers of marine sediments (Berner 1970, Howarth & Jørgensen 1984) and high concentrations of reduced sulfur near the sediment-water interface are generally considered to be diagenetically produced (Berner 1970; Sweeney & Kaplan 1980; Goldhaber & Kaplan 1980). However, it is likely that most, if not all of the surface layer pyrite in the Eastern Scheldt sediments if of detrital origin.

The recent sediments in the Eastern Scheldt mainly consist of material from eroding, older marine deposits, containing FeS_2. Pyrite has been detected in suspended matter (Kooistra 1981) and in the oxidizing surface layers of salt marshes (Oenema 1988a). In-situ pyrite formation in the surface layers of recent sediments cannot totally be ruled out, but probably did not exceed 30% of the total FeS_2 concentration. This figure was estimated from the small difference between the FeS_2 concentrations in the recent channel bottom sediments and the newly-deposited surface sediments of salt marshes. In the marshes the detrital FeS_2 was oxidized in the surface layers, and its concentration decreased from 40–80 μM at 0–1 cm to $< 8\ \mu$M S-FeS_2 cm^{-3} at 5–12 cm (Oenema 1988a).

Conclusions

The results of this study indicate that the upward diffusion of SO_4^{2-} from the underlying sandy sediments significantly contributed to the total influx of SO_4^{2-} into mussel banks. The subsurface influx of SO_4^{2-}, in combination with

increased apparent sediment diffusivities, prevented the pore waters from a total exhaustion of SO_4^{2-}, especially in summer when reduction rates were high. The mussel banks were removed by dredging after a growth period of 1–2 years, so that the sandy subsurface sediments became exposed temporarily. This allowed a rapid replenishment of the sulfate-depleted pore waters before a new mussel culture started. In the recently abandoned channels, the siltation was continuous and there the effect of the upward diffusion of SO_4^{2-} from the sandy subsurface gradually faded away.

The sedimentation rate was the chief determinant of the rate of sulfate reduction. In the most rapidly accreting channels SO_4^{2-} was exhausted below a depth of 15–50 cm. Pore waters of these sediments were saturated with CH_4 at depth greater than about 10 cm.

Acid volatile sulfides (AVS) and pyrite (FeS_2) accumulated both at a rate of 4–7.5 moles S $m^{-2} yr^{-1}$ in the highly reducing sediments. AVS was the major end product of in-situ reduced S. In thick mussel banks apparently all easily reducible iron oxyhydroxides were converted into acid volatile iron monosulfides. The steep dissolved ΣS profiles in the surface layers indicate that also a large portion of the in-situ reduced S diffused upward to the sediment surface, where it probably oxidized. Most, if not all, of the pyrite in the recent sediments was of detrital origin. The in-situ pyrite formation via AVS intermediates was very slow, since no change in the depth profiles of AVS, FeS_2 and Fe_{ox} was found.

The upward SO_4^{2-} diffusion from the sand layers below organically-rich debris, the sedimentation of detrital pyrite and the apparent absence of in-situ pyrite formation make mussel culture areas and abandoned channels in the Eastern Scheldt unique environments.

Acknowledgements

I would like to thank Peter van der Wege, Ko Siereveld and Hans Verkooien for their valuable help in sampling abandoned channels, and Mark van Alphen for assistance with the sulfide analysis. Chloride and sulfate analysis were carried out at the laboratory of Rijkswaterstaat, Tidal Waters Division, Middelburg. Also acknowledged are the helpful advice of Dr Van Steen with the transient-state model and Drs B.B. Jørgensen, G.T.M. Van Eck, F.R. Moormann and two anonymous reviewers for critical remarks on earlier versions of this manuscript. This research was carried out at the Institute of Earth Sciences, University of Utrecht and supported by the Delta Department of the Ministry of Transport and Public Works.

References

Aller RC (1980) Diagenetic processes near the sediment-water interface of Long Island Sound. II Fe and Mn. Adv. Geophys. 22: 351–415

Bassett J, Denney RC, Jeffery GH & Mendham J (1978) Vogel's Textbook of Quantitative Inorganic Analysis. Longman Inc. New York, 925 pp

Begheyn LTh, Van Breeman N & Veldhorst EJ (1978) Analysis of sulfur compounds in acid sulfate soils and other recent marine soils. Comm. Soil Sc. Plant Anal. 9: 873–882

Berner RA (1964) An idealized model of dissolved sulfate distribution in recent sediments. Geochim. Cosmochim. Acta 28: 1497–1503

——— (1970) Sedimentary pyrite formation. Am. J. Sci. 268: 1–23

——— (1978) Sulfate reduction and the rate of deposition of marine sediments. Earth Planet. Sc. Lett. 37: 492–498

——— (1980) Early diagenesis, a theoretical approach. Princeton University Press, New Jersey

——— (1984) Sedimentary pyrite formation; an update. Geochim. Cosmochim. Acta 48: 605–615

Berner RA & Westrich JT (1985) Bioturbation and the early diagenesis of carbon and sulfur. Am. J. Sci. 285: 193–206

Boudreau BP & Westrich JT (1984) The dependence of bacterial sulfate reduction on sulfate concentration in marine sediments. Geochim. Cosmochim. Acta. 48: 2503–2516

Chanton JP & Martens CS (1985) The effects of heat and stannous chloride addition on the active distillation of acid volatile sulfide from pyrite-rich marine sediment samples. Biogeochem. 1: 375–382

Chanton JP, Martens CS & Goldhaber MB (1987) Biogeochemical cycling in an organic rich coastal marine basin. 7. Sulfur mass balance, oxygen uptake and sulfide retention. Geochim. Cosmochim. Acta. 51: 1187–1199

Claypool GE & Kaplan IR (1974) The origin and distribution of methane in marine sediments. In: Kaplan IR (Ed) Natural Gases in Marine Sediments (pp 99–139) Plenum

Crill PM & Martens CS (1987) Biogeochemical cycling in an organic-rich coastal marine basin. 6. Temporal and spatial variations in sulfate reduction rates. Geochim. Cosmochim. Acta 51: 1175–1186

Devol AH, Anderson JJ, Kuivila K & Murray JW (1984) A model for coupled sulfate reduction and methane oxidation in the sediments of Saanich Inlet. Geochim. Cosmochim. Acta 48: 993–1004

Dew PM & Walsh JE (1981) A set of library routines for solving parabolic equations in one space variable. ACM Trans. Math. Software, Vol 7: 295–314

Goldhaber MB & Kaplan IR (1975) Controls and consequences of sulfate reduction in recent marine sediments. Soil Sci. 119: 42–55

Goldhaber MB & Kaplan IR (1980) Mechanisms of sulfur incorporation and isotope fractionation during early diagenesis in sediments of the Gulf of California. Mar. Chem. 9: 95–143

Gilboa-Garber N (1971) Direct spectrofotometric determination of inorganic sulfide in biological materials and in other complex mixtures. Anal. Biochem. 43: 129–133

Hesslein RH (1976) An in-situ sampler for close interval pore studies. Limnol. Oceanogr. 21: 912–914

Hordijk CA, Hagenaars CPMM & Cappenberg ThE (1985) Kinetic studies of bacterial sulfate reduction in freshwater sediments by high-pressure liquid chromatography and micro-distillation. Appl. Environ. Microbiol. 49: 434–440

Howarth RW (1984) The ecological significance of sulfur in the energy dynamics of saltmarsh

and coastal marine sediments. Biogeochem. 1: 5–27
Howarth RW & Jørgensen BB (1984) Formation of ^{35}S-labelled elemental sulfur and pyrite in coastal marine sediments (Limfjorden and Kysing Fjord, Denmark) during short-term $^{35}SO_4^{2-}$ reduction measurements. Geochim. Cosmochim. Acta 48: 1807–1818
Jørgensen BB (1977) The sulfur cycle of a coastal marine sediment. Limnol. Oceanogr. 22: 814–832
——— (1978) A comparison of methods for the quantification of bacterial sulfate reduction in coastal marine sediments. II Calculations from mathematical models. Geomicrobiol. J. 1: 29–47
——— (1982) Mineralisation of organic matter in the sea-bed; the role of SO_4^{2-} reduction. Nature. 296: 643–645
Klump JV & Martens CS (1981) Biogeochemical cycling in an organic-rich coastal marine basin. 2. Nutrient sediment-water exchange processes. Geochim. Cosmochim. Acta 45: 101–121
Knoester M, Visser J, Bannink BA, Colijn CJ & Broeders WPA (1984) The Eastern Scheldt project. Wat. Sci. Techn. 16: 51–77
Kooistra MJ (1981) The determination of Fe, Mn, S and P in thin sections of recent marine intertidal sediments in S.W. Netherlands by SEM-EDXRA. In: Bisdom EBA (Ed) Submicroscopy of Soils and Weathered Rocks (pp 217–236) Pudoc, Wageningen
Li YH & Gregory S (1974) Diffusion of ions in seawater and deep sea sediments. Geochim. Cosmochim. Acta 38: 703–714
Luther III, GW, Giblin AE & Varsolona R (1985) Polarographic analysis of sulfur species in marine pore waters. Limnol. Oceanogr. 30: 727–736
Lyons WB & Gaudette HE (1979) Sulfate reduction and the nature of organic matter in estuarine sediments. Org. Geochem. 1: 151–155
Martens CS & Klump JV (1980) Biogeochemical cycling in an organic rich coastal marine basin. 1. Methane sediment-water exchange processes. Geochim. Cosmochim. Acta 44: 471–490
Merks AGA & Sinke JJ (1981) Application of an automated method for dissolved sulfate analysis to marine and brackish waters. Mar. Chem. 10: 103–108
Morse JW & Cornwell JC (1987) Analysis and distribution of iron sulfide minerals in recent marine sediments. Mar. Chem. 22: 55–69
Oenema O (1988a) Early diagenesis in recent fine-grained sediments in the Eastern Scheldt. PhD. diss., Univ. Utrecht, 223 pp
——— (1988b) Diagenesis in subrecent marine sediments in the Eastern Scheldt, Southwest Netherlands. Neth. J. Sea Res. 22: 253–265
——— (1989) Distribution and cycling of fine-grained sediments in the Eastern Scheldt, Southwest Netherlands. Geol. Mijnbouw 68: 189–200
Pyzik AJ & Sommer SE (1981) Sedimentary iron monosulfides: kinetics and mechanism of formation. Geochim. Cosmochim. Acta 45: 687–698
Rickard DT (1975) Kinetics and mechanism of pyrite formation at low temperature. Am. J. Sci. 275: 636–652
Schwertmann U (1964) Differenzierung der Eisenoxide des Bodens durch Extraction mit ammoniumoxalat-Lösung. Z. Pflanzenernähr. Dung. Bodenkunde. 105: 194–203
Skyring GW (1987) Sulfate reduction in coastal ecosystems. Geomicrobiol. J. 5: 295–374
Sweeney RE & Kaplan IR (1973) Pyrite framboid formation: Laboratory synthesis and marine sediments. Econ. Geol. 68: 618–634
Toth DJ & Lerman A (1977) Organic matter reactivity and sedimentation rates. Am. J. Sc. 277: 465–485
Ullmann WJ & Aller RC (1982) Diffusion coefficients in nearshore marine sediments. Limnol. Oceangr. 27: 552–556

Westrich JT & Berner RA (1984) The role of sedimentary organic matter in bacterial sulfate reduction: The G model tested. Limnol. Oceanogr. 29: 236–249

Zall MD, Fisher D & Garner MD (1956) Photometric determination of chlorides in water. Anal. Chem. 28: 1665–1668